similar discrepancies in other values such as $O_3$ are not improved[36]. Rather, the importance of this test is to show that the correlation and slope are robust features at high latitudes. The ATMOS data shown in Fig. 2*c* further suggest that large-scale, advective transport of air parcels containing >80 p.p.b.v. $N_2O$ from mid-latitudes to the polar regions in the complete absence of horizontal mixing would still produce a linear correlation. These data are in fair agreement with the model, which clearly shows a linear correlation over a similar range of $NO_y$ and $N_2O$ values in Fig. 2*c*.

Evidence for the importance of photochemistry at low latitudes and poleward transport in creating the model ECE field is provided in Fig. 3*c*, *d*. In Fig. 3*c*, the net photochemical production rates of $NO_y$ at noon are shown as an example of the spatial distribution of the conversion process. The rate maximizes in the tropics near 35 km and decreases to zero in polar night. The destruction rate for $N_2O$ shows a similar pattern[37]. The latitude and altitude dependence of the rate depends primarily on the distribution of solar ultraviolet. Model contours of the resulting $NO_y$ mixing ratio show a similar symmetric distribution with a maximum near 23 p.p.b.v. between 35 and 40 km in the tropics. At the maximum $NO_y$ production rate in the tropics, 20 p.p.b.v. of $NO_y$ is formed in ~150 days, indicating that the timescale for transport into and out of this region must be of the same order.

By comparing the rates of net production of $NO_y$ and destruction of $N_2O$, a local instantaneous conversion efficiency of $N_2O$ to $NO_y$ can be calculated at each model grid point. Between 28 and 41 km, the contours are nearly horizontal over a broad latitude range, with values <15% (Fig. 3*d*). Values in the region of maximum $NO_y$ production are 10 ± 2%, comparable to the 7% value observed at high latitudes. The largest instantaneous efficiencies are found at high latitudes where the maximum value of 116% corresponds to twice the branching ratio to NO in reaction (1). Observed ECE values are near ~7% and minimum net production rates indicate that high latitudes cannot be the region of $N_2O$ conversion.

The link between model ECE values in Fig. 3*a* and the steady-state fields in Fig. 3*c*, *d* is transport and mixing. The general features of the zonally averaged transport are (see Fig. 3*d*): air rises in the tropics, moves poleward throughout the low and middle stratosphere, and descends at high latitudes[31,38,39]. Horizontal and vertical eddy mixing are superimposed on this mean circulation. Horizontal mixing typically dominates vertical mixing in the lower stratosphere. Thus, transport of air occurs from the region of maximum photochemical production into the region of observation. Differences must exist between the instantaneous conversion efficiency and the observed ECE values, in part because of the residence time of air in the $NO_y$ production region and mixing of air from the production region with air that has experienced greater $NO_y$ loss at higher altitudes or less $N_2O$ loss at lower altitudes. The linearity of the correlation over a wide range of $N_2O$ values suggests that mixing must be effective. The long photochemical lifetimes of both species in the lower stratosphere imply, however, that mixing timescales need only exceed the timescale for descent from the $NO_y$ loss region ($N_2O$ values <50 p.p.b.v.) for a linear correlation to be maintained. Thus, the understanding of the model ECE field provided by Fig. 3 provides a high level of confidence in a linear correlation as a reference state for $NO_y$ and $N_2O$. □

Received 31 January; accepted 25 April 1990.


1. Fahey, D. W. *et al. J. geophys. Res.* **94,** 16665–16681 (1989).
2. Proffitt, M. H., Fahey, D. W., Kelly, K. K. & Tuck, A. F. *Nature* **342,** 233–237 (1989).
3. Poole, L. R. *et al. Geophys. Res. Lett.* **17,** 537–540 (1990).
4. Jones, R. L. *et al. J. geophys. Res.* **94,** 11529–11558 (1989).
5. Tuck, A. F., Watson, R. T., Condon, E. P., Margitan, J. J. & Toon, O. B. *J. geophys. Res.* **94,** 11181–11222 (1989).
6. Turco, R., Plumb, A. & Condon, E. *Geophys. Res. Lett.* **17,** 313–316 (1990).
7. Loewenstein, M., Podolske, J. R., Chan, K. R. & Strahan, S. E. *J. geophys. Res.* **94,** 11589–11598 (1989).
8. Tuck, A. F. *J. geophys. Res.* **94,** 11687–11737 (1989).
9. Murphy, D. M. *et al. J. geophys. Res.* **94,** 11669–11685 (1989).
10. Toon, G. C. *et al. J. geophys. Res.* **94,** 16571–16596 (1989).
11. Kawa, S. R., Fahey, D. W., Anderson, L. C., Loewenstein, M. & Chan, K. R. *Geophys. Res. Lett.* **17,** 485–488 (1990).
12. Anderson, J. G., Brune, W. H. & Proffitt, M. H. *J. geophys. Res.* **94,** 11465–11479 (1989).
13. Brune, W. H., Toohey, D. W., Anderson, J. G. & Chan, K. R. *Geophys. Res. Lett.* **17,** 505–508 (1990).
14. Proffitt, M. H. *et al. J. geophys. Res.* **94,** 11437–11448 (1989).
15. Fahey, D. W. *et al. J. geophys. Res.* **94,** 11299–11315 (1989).
16. Kelly, K. *et al. J. geophys. Res.* **94,** 11317–11357 (1989).
17. Toon, O. B., Hamill, P., Turco, R. P. & Pinto, J. *Geophys. Res. Lett.* **13,** 1284–1287 (1986).
18. McCormick, M. P., Trepte, C. R. & Pitts, M. C. *J. geophys. Res.* **94,** 11241–11251 (1989).
19. Watterson, I. G. & Tuck, A. F. *J. geophys. Res.* **94,** 16511–16525 (1989).
20. Arnold, F., Schlager, H., Hoffmann, J., Metzinger, P. & Spreng, S. *Nature* **342,** 493–497 (1989).
21. Arnold, F. & Knop, G. *Nature* **338,** 746–749 (1989).
22. Fahey, D. W. *et al. Nature* **344,** 321–324 (1990).
23. Galbally, I. E. *et al. Q. Jl R. met. Soc.* **112,** 775–809 (1986).
24. Gunson, M. R. *et al. J. geophys. Res.* (in the press).
25. Russell, J. M. III *et al. J. geophys. Res.* **93,** 1718–1736 (1988).
26. Jackman, C. H., Frederick, J. E. & Stolarski, R. S. *J. geophys. Res.* **85,** 7495–7505 (1980).
27. *Chemical kinetics and photochemical data for use in stratospheric modeling, Evaluation # 8, JPL Publ. 87-41* (NASA, Jet Propulsion Laboratory, Pasadena, 1987).
28. Greenblatt, G. D. & Ravishankara, A. R. *J. geophys. Res.* **95,** 3539–3548 (1990).
29. Hübler, G., Fahey, D. W., Ridley, B. A., Gregory, G. & Fehsenfeld, F. C. *J. geophys. Res.* (submitted).
30. Butler, J. H., Elkins, J. W., Thompson, T. M. & Egan, K. B. *J. geophys. Res.* **94,** 14865–14877 (1989).
31. WMO Global Ozone Research and Monitoring Project, *Atmospheric Ozone Report 16* (World Meteorological Organization, Geneva, 1985).
32. Brasseur, G. & Solomon, S. *Aeronomy of the Middle Atmosphere* 2nd edn (Reidel, Dordrecht, 1986).
33. Podolske, J. R., Loewenstein, M., Strahan, S. E. & Chan, K. R. *J. geophys. Res.* **94,** 16767–16772 (1989).
34. Loewenstein, M., Podolske, J. R., Chan, K. R. & Strahan, S. E. *Geophys. Res. Lett.* **17,** 477–480 (1990).
35. Ko, M. K. W., Tung, K. K., Weisenstein, D. K. & Sze, N. D. *J. geophys. Res.* **90,** 2313–2329 (1985).
36. Chipperfield, M. P. & Pyle, J. A. *Geophys. Res. Lett.* **15,** 875–878 (1988).
37. Solomon, S. & Garcia, R. R. *J. geophys. Res.* **89,** 11633–11644 (1984).
38. Garcia, R. R. & Solomon, S. *J. geophys. Res.* **88,** 1379–1400 (1983).
39. Pawson, S. & Harwood, R. S. *Q. Jl R. met. Soc.* **115,** 807–840 (1989).
40. Loewenstein, M., Podolske, J. R. & Strahan, S. E. *Geophys. Res. Lett.* **17,** 481–484 (1990).
41. Johnston, H. S., Serang, O. & Podolske, J. *J. geophys. Res.* **84,** 5077–5082 (1979).
42. Solomon, S., Kiehl, J. T., Garcia, R. R. & Grose, W. *J. atmos. Sci.* **43,** 1603–1617 (1986).


ACKNOWLEDGEMENTS. We thank R. R. Garcia, I. S. A. Isaksen, K. K. Kelly, M. K. W. Ko, M. B. McElroy, M. J. Prather, D. M. Murphy, M. H. Proffitt and A. F. Tuck for discussions, and B. W. Gandrud, D. Baumgardner, J. E. Dye, G. V. Ferry and M. R. Gunson for the use of their data. This research was supported by NASA, the Chemical Manufacturers Association and the NOAA.

# Biological removal of dimethyl sulphide from sea water

**Ronald P. Kiene* & Timothy S. Bates†**

* University of Georgia Marine Institute, Sapelo Island, Georgia 31327, USA
† National Oceanic and Atmospheric Administration, Pacific Marine Environmental Laboratory, 7600 Sand Point Way, NE, Seattle, Washington 98115, USA

**DIMETHYL sulphide (DMS) is an important sulphur-containing trace gas in the atmosphere. It is present in oceanic surface waters at concentrations sufficient to sustain a considerable net flux of DMS from the oceans to the atmosphere, estimated to comprise nearly half of the global biogenic input of sulphur to the atmosphere[1]. DMS emitted from the oceans may be a precursor of tropospheric aerosols and of cloud condensation nuclei in the remote marine atmosphere, thereby affecting the Earth's radiative balance and thus its climate[2–4]. Relatively little is known, however, about the biogeochemical and physical processes that control the concentration of DMS in sea water. Here we present data from incubation experiments, carried out at sea, which show that DMS is removed by microbial activity. In the eastern, tropical Pacific Ocean, DMS turnover is dominated by biological processes, with turnover times for biological DMS removal generally more than ten (3–430) times faster than turnover by ventilation to the atmosphere. Thus biological consumption of DMS seems to be a more important factor than atmospheric exchange in controlling DMS concentrations in the ocean, and hence its flux to the atmosphere. These results have significant implications for climate feedback models involving DMS emissions[3], and highlight the importance of the microbial food web in oceanic DMS cycling.**

We carried out experiments aboard the NOAA *Discoverer* as it sailed from 20° N to 23° S between 105° W and 110° W in February 1989. In freshly collected surface seawater samples,

TABLE 1 Biological consumption and sea–air exchange of dimethylsulphide

| Sample location | Depth (m) | Incubation temperature* (°C) | Dissolved DMS† (nM) | Biological consumption rate (nM $d^{-1}$) | $\tau_{bio}$ (d)‡ | DMS column burden (μmol $m^{-2}$) | Air–sea exchange rate (μmol $m^{-2}$ $d^{-1}$) | $\tau_{atmos}$ (d)‡ | $\frac{\tau_{atmos}}{\tau_{bio}}$ |
|---|---|---|---|---|---|---|---|---|---|
| 20.5° N, 107.2° W | 5 | 22 | 3.7 | 5.1 | 0.7 | ND | — | — | — |
| 14.8° N, 105.0° W | 5 | 27 | 1.5 | 1.4 | 1.1 | ND | — | — | — |
| 10.5° N, 105.6° W | 5 | 28 | 2.8 | 1.7 | 1.6 | 219 | 9.4 | 23 | 15 |
| 4.7° N, 108.5° W | 5 | 26 | 10.3 | 18.0 | 0.6 | 266 | 24.0 | 11 | 12 |
| 1.1° S, 110° W | 5 | 26 | 4.4 | 3.7 | 1.2 | 259 | 0.5 | 520 | 430 |
| 7.4° S, 108.3° W | 5 | 26 | 2.4 | 1.1 | 2.2 | 306 | 6.0 | 51 | 23 |
| 15.3° S, 105° W | 5 | 25 | 6.0 | 1.3 | 4.6 | 503 | 36.0 | 14 | 3 |
| 22.3° S, 105° W | 40§ | 24 | 0.8 | 1.1 | 0.7 | 141 | 5.3 | 27 | 38 |

Biological turnover rates were determined by measuring the rate of DMS accumulation in the presence of chloroform and subtracting the rate of DMS accumulation in untreated samples. Duplicate bottles of each treatment were used. At least four time points over a 12-h period were used to calculate rates. Biological turnover times were calculated by dividing the measured DMS concentration in sample bottles by the DMS consumption rate in those samples. Turnover rates due to atmospheric exchange were calculated by dividing the column burden of DMS in the mixed layer, determined from depth profiles, by the estimated flux of DMS to the atmosphere[1]. ND, no data.

* Incubation temperatures were within 1 °C of the *in situ* temperature.

† DMS concentrations measured in first reading of untreated samples; up to 2 h after collection.

‡ $\tau_{bio}$ is the biological turnover time and $\tau_{atmos}$ is the atmospheric turnover time.

§ Collected by hydrocast using Niskin bottle.

incubated with and without DMS additions, DMS concentrations increased for a time and then decreased (Fig. 1). The initial increases in DMS were probably due to the decomposition of endogenous dimethylsulphoniopropionate (DMSP), which is believed to be the principal biogenic precursor of DMS in the ocean[5–7]. Both chloroform (an inhibitor of $C_1$ metabolism and possible general biocide) and a mixture of the broad-spectrum antibiotics—chloramphenicol and tetracycline (CAP-TET)—prevented the loss of DMS. These results indicate that DMS is biologically consumed by microbial metabolism in sea water.

Several possibilities exist for the aerobic metabolism of DMS, including use by methylotrophs and chemolithotrophs[8–10]. DMS could be also oxidized to dimethylsulphoxide (DMSO) by organisms as yet uncharacterized[11,12]. Unfortunately, little or no information exists as to which of these processes are responsible for DMS removal in the sea.

Chloroform ($CHCl_3$) is a known inhibitor of $C_1$ metabolism[13], therefore it is not surprising that it inhibited the consumption of DMS in sea water. In samples to which we added $CHCl_3$, DMS always accumulated at a higher rate than in untreated samples (Fig. 2) because DMS consumption is inhibited by chloroform, whereas its production from dissolved and particulate DMSP is not affected by the inhibitor (R.P.K., manuscript in preparation). The increased rate of DMS accumulation in the presence of chloroform therefore represents an estimate of its natural removal rate.

We have estimated DMS removal rates and biological turnover times for surface water samples collected in the eastern Pacific Ocean (Table 1). DMS consumption rates during incubations in the dark ranged from 1.1 nM $d^{-1}$ to 18.0 nM $d^{-1}$ yielding turnover times $\tau_{bio}$ ranging from 0.6 to 4.6 d. The high DMS concentration and consumption rate at 4.7° N were probably a result of increased productivity caused by nearby equatorial upwelling. DMS consumption rates were more strongly correlated with DMS concentrations ($r^2 = 0.741$; $n = 8$) than with particulate DMSP concentrations ($r^2 = 0.337$; $n = 7$).

Sea–air exchange of DMS, calculated from DMS column burdens, wind speed and sea surface temperature[1], ranged from 0.5 to 36 μmol $m^{-2}$ $d^{-1}$ for these sites, yielding turnover times $\tau_{atmos}$ ranging from 11.3 to 518 d for DMS in the mixed layer. The ratios of $\tau_{atmos}$ to $\tau_{bio}$ (surface samples only) ranged from a low of 3 at 15° S to a high of 430 near the Equator at 1° S. The exceptionally small contribution of atmospheric exchange to DMS cycling at 1° S was due to calm winds which resulted in very little surface ventilation.

Removal of DMS from sea water by mechanisms other than sea–air exchange has been suggested by several investigators[5,14–17], but no direct evidence has previously been

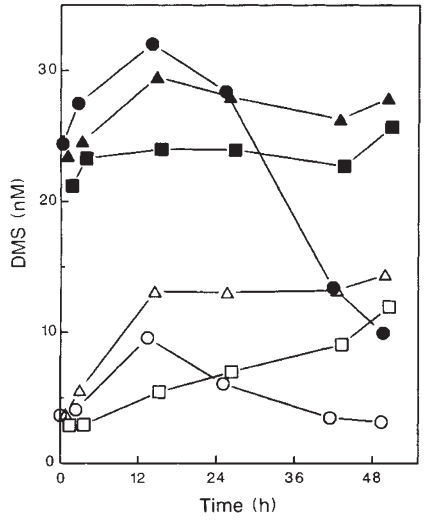


FIG. 1 DMS concentrations as a function of time in water samples incubated with or without spikes of DMS. Inhibitors were added to prevent microbial metabolism. Symbols: (○) no addition; (△) chloroform (500 μM); (□) antibiotics, chloramphenicol and tetracycline (125 mg $l^{-1}$ and 75 mg $l^{-1}$); (●) DMS; (▲) DMS + chloroform; (■) DMS + antibiotics. Data represent the means of duplicate bottles for each treatment and exhibited a range of ~10%. Water was collected while underway, from a pumping system located ~5 m under the bow of the ship. The station location was 20.5° N 107.2° W. Water samples (130 ml) were incubated in 140-ml silanized glass, acid-rinsed serum bottles sealed with teflon-faced septa and held in the dark at *in situ* temperature (22 °C). Subsamples for DMS analysis were taken periodically by removing the seal and taking up 5 ml with a teflon tube attached to a glass syringe. The water sample was then gently passed through a glass-fibre filter (Whatman GF/F) and introduced into a sparging system where the DMS was stripped from solution, and concentrated on a trap immersed in liquid argon. The cold-trap was replaced by hot water and the sulphur gases introduced into a gas chromatograph equipped with a Carbopack BHT 100 (2 m long, 1/8" diameter teflon) column and flame-photometric detector. DMS standards were prepared in ethylene glycol and a ship-board intercalibration with the NOAA/PMEL system[2] yielded agreement within 10%.

presented for biological consumption of DMS in natural ocean water. Our data indicate that, in most cases, biological removal of DMS in the surface ocean is much more important than DMS removal by ventilation. Even if our estimates of biological consumption are too large by a factor of 10, this process would still dominate over atmospheric exchange in all but one case (15 °S).

Other potential sinks for DMS in surface sea water (Fig. 3) include photochemical oxidation[16] and particle adsorption with subsequent vertical transport to the deep sea[17]. Both of these processes are poorly understood. The only estimates that exist for these processes[16,17] indicate that they are less significant on a global scale than atmospheric exchange of DMS, and therefore would yield longer turnover times than biological reactions. Because our data set is small, and covers only tropical and subtropical waters, further research is needed to compare the relative importance of biological consumption to other DMS sinks.

The fact that DMS is cycled quickly in sea water by biological reactions raises interesting questions regarding the possible role of DMS in climate feedback mechanisms. Predicting how DMS flux will change as a result of climate change, however, is a difficult task. The primary factors that control DMS fluxes are the sea–air transfer coefficient and the DMS concentration in surface water[1]. The sea–air transfer coefficient is dependent on physical factors such as temperature and wind speed whereas the DMS concentration is a function of physical and biological processes related to its sources and sinks (Fig. 3).

Gross DMS production is linked to the production of its biogenic precursor DMSP which is produced by a subset of the algal population[6,7,18]. Climatic controls on the phytoplankton, expressed through physical factors such as temperature, light and nutrient regimes, would be expected to influence the structure of the algal population (the biomass, productivity, species composition and size distribution, for example), as well as the total DMSP production by this population. Although it seems that DMS concentration is related to total DMSP (dissolved and particulate)[6,7], there are insufficient data to extend this conclusion to all ocean environments. DMS concentrations may not necessarily follow the total DMSP content of sea water if microbial consumption of DMS is tightly coupled with its production.

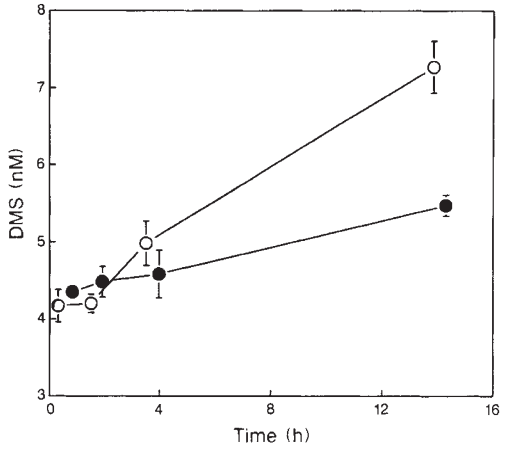


FIG. 2 Effect of chloroform (500 μM) on the concentration of DMS in seawater samples incubated in the dark at *in situ* temperature (25 °C). Symbols: (●) untreated; (○) added chloroform. Data points represent the mean DMS concentration for three separate bottles. Vertical bars indicate one standard deviation. Higher or lower concentrations of chloroform produced a smaller stimulation (data not shown). The stimulation of DMS accumulation by chloroform varied in samples collected from different depths but was not significantly correlated with particulate DMSP. In separate experiments, chloroform did not significantly affect bacterial numbers or the disappearance of particulate or dissolved DMSP during 24-h dark incubations. The station location was 1.1° S 110° W.

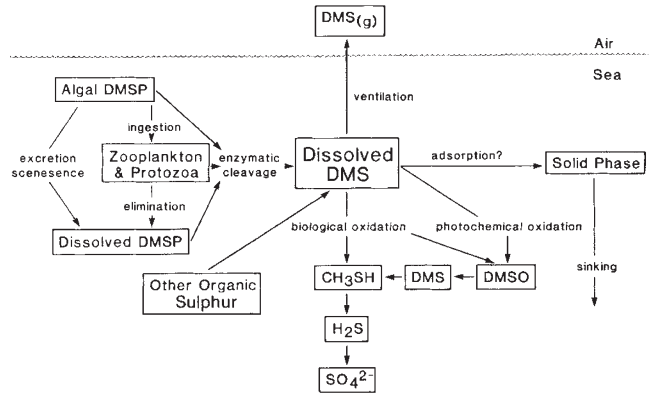


FIG. 3 Diagram illustrating the known sources and sinks for DMS in the surface ocean. Processes involving DMS production from algal DMSP are based on refs 15 and 19. The potential adsorption and photochemical destruction of DMS are based on the work of Brimblecoombe and Shooter[16] and Shooter and Brimblecoombe[17]. The possible contribution of other organic sulphur compounds to DMS production is based on work by Kiene and Capone[21]. Products of DMS metabolism are those reported for methylotrophic and chemolithotrophic metabolism[9,10]. Diffusion and advection are ignored.

The impact of grazing on algal and bacterial populations must also be included in considerations of climate-change effects on DMS. Dacey and Wakeham[19] have shown that an important pathway for DMS production is likely to be through organisms that graze DMSP-producing algae, and those that either metabolize DMSP themselves or liberate dissolved DMSP ($DMSP_{diss}$). Assuming that conversion of $DMSP_{diss}$ to DMS is relatively rapid (R.P.K., manuscript in preparation), gross DMS production will be a function of the grazing pressure on the DMSP-producing algal population, which may or may not be the same as the grazing pressure on the algal population as a whole. This is likely to depend on the size classes of the DMSP-producing algae and on any preference or avoidance of these algae by grazers. These latter points could be critical to our understanding of DMS cycling if the mechanisms of DMS production differ in systems dominated by large zooplankton grazers compared to those dominated by nanoplanktonic grazers.

Similarly, if DMS and $DMSP_{diss}$ metabolism occur in the bacterial populations, these activities will probably be controlled by the concentrations of the respective substrates and by bacterial mortality (most likely through nanoplanktonic grazing and possibly by virus infection[20]). Thus, DMS concentrations are intimately connected to the structure of the marine pelagic food web, particularly the microbial loop. Plankton populations that interact to affect DMS concentrations (such as zooplankton, algae, heterotrophic nanoplankton and bacteria) are not likely to be in a steady state, and therefore predicting effects of climate change on DMS will involve complex models that consider ecological interactions as well as physical and chemical factors. Our ability to use such models will require far greater understanding of individual processes than we now have. □

Received 13 February; accepted 18 April 1990.

1. Andreae, M. O. in *The Role of Air–Sea Exchange in Geochemical Cycling* (ed Buat-Menard, P.) 331–362 (Reidel, Dordrecht, 1986).
2. Bates, T. S., Charlson, R. J. & Gammon, R. G. *Nature* **329,** 319–321 (1987).
3. Charlson, R. J., Lovelock, J. E., Andreae, M. O. & Warren, S. G. *Nature* **326,** 655–661 (1987).
4. Savoie, D. L. & Prospero, J. M. *Nature* **339,** 685–687 (1989).
5. Andreae, M. O. & Barnard, W. R. *Mar. Chem.* **14,** 267–279 (1984).
6. Turner, S. M., Malin, G. & Liss, P. S. *Limnol. Oceanogr.* **33,** 364–375 (1988).
7. Iverson, R. L., Nearhoof, F. L. & Andreae, M. O. *Limnol. Oceanogr.* **34,** 53–67 (1989).
8. De Bont, J. A. M., Van Dijken, J. P. & Harder, W. *J. gen. Microbiol.* **127,** 315–323 (1981).
9. Suylen, G. M. H., thesis, Technical University of Delft (1988).

10. Kelly, D. P. in *The Nitrogen and Sulphur Cycles, Soc. gen. Microbiol. Symp.* 42 (eds Cole, J. & Ferguson, S.) 65–98 (Cambridge University Press, 1988).
11. Andreae, M. O. *Limnol. Oceanogr.* **25,** 1054–1063 (1980).
12. Taylor, B. F. & Kiene, R. P. in *Biogenic Sulphur in the Environment* (eds Saltzman, E. & Cooper, W. J.) 202–221 (Am. chem. Soc., Washington, DC, 1989).
13. Bauchop, T. *J. Bact.* **94,** 171–175 (1967).
14. Andreae, M. O. *Limnol. Oceanogr.* **30,** 1208–1218 (1985).
15. Wakeham, S. H., Howes, B. L., Dacey, J. W. H., Schwarzenbach, R. P. & Zeyer, J. *Geochim. cosmochim. Acta* **51,** 1675–1684 (1987).
16. Brimblecombe, P. & Schooter, D. *Mar. Chem.* **19,** 343–353 (1986).
17. Shooter, D. & Brimblecombe, P. *Deep Sea Res.* **36,** 577–585 (1989).
18. Keller, M. D., Bellows, W. K. & Guillard, R. R. L. in *Biogenic Sulphur in the Environment* (eds Saltzman, E. & Cooper, W. J.) (Am. chem. Soc., New York, 1987).
19. Dacey, J. W. H. & Wakeham, S. G. *Science* **233,** 1314–1316 (1986).
20. Proctor, L. M. & Fuhrman, J. A. *Nature* **343,** 60–62 (1990).
21. Kiene, R. P. & Capone, D. G. *Microbiol Ecol.* **15,** 275–291 (1988).

ACKNOWLEDGEMENTS. We thank the scientists and crew aboard the *Discoverer*. We also thank E. Sherr and B. Sherr for comments. This work was supported by the NSF and The University of Georgia Marine Institute (R.P.K.) and by the NOAA Radiatively Important Trace Species Program (T.S.B.).

# A record from Lake Cardiel of climate change in southern South America

**Scott Stine & Mary Stine**

Lamont-Doherty Geological Observatory, Palisades, New York 10964, USA

**SOUTHERN South America, the only continental land mass lying between 38° S and the Antarctic Circle, presents a rare opportunity to reconstruct terrestrial records of palaeoclimate in an area that is subject to shifts of polar and mid-latitude wind and pressure belts. In the bulk of this region (Patagonia) are many hydrographically closed lakes which, despite the palaeoclimatic significance of the region and the proven utility of lake level records in reconstructing past climates[1,2], have escaped detailed study. Using sedimentary and geomorphic evidence, together with $^{14}C$ dating, we present here a detailed lake level record for Lake Cardiel (Fig. 1). The highest level of the past >21,000 years occurred at about 9,780 BP, reminiscent of tropical lakes rather than those in northern mid-latitudes[1,2]. The Lake Cardiel record corroborates and clarifies the timing of the wetness record inferred from pollen studies in Patagonia.**

Lake Cardiel is a large (360 km$^2$) water body that occupies a xeric ~4,000-km$^2$ closed depression east of and hydrographically isolated from the Andes in southern Argentina (Fig. 1). Strand lines encircle the lake at elevations as much as 75 m above today's shoreline, attesting to former higher levels[3]. These appear to be neither warped nor faulted. Littoral embankments at and below the +55-m level are prominent. They are composed of unvarnished clasts and are breached only where they intersect the most active streams and arroyos. By contrast those above +55-m are subdued, deeply dissected, only traceable around <30% of the lake and often are covered with stone pavements composed of varnished beach shingle, indicating that they are at least several times older than the lower ones.

In the course of the fluctuations that deposited the embankments the lake alternately embayed and abandoned the lower reaches of the tributary canyons. During transgressions and highstands the streams built deltas in the canyons, whereas at low lake levels deltas formed beyond the canyon mouths. In response to the modern drop in lake level the streams have incised their deltas, exposing alternating sequences of transgressive and regressive deposits with intervening soils. In some cases these can be traced for thousands of metres up and down stream; in several instances individual sequences terminate at a buried or surface strand line that marks the terminal elevation of a transgression.

Datable materials, including tufa (lacustrine deposits of $CaCO_3$) and organic detritus, abound in these sections. The tufa deposits occur as beachrock (tufa-cemented littoral sediments), and as rinds that coat the outside of littoral cobbles and boulders. We believe that $^{14}C$ assays on these littoral tufa deposits provide reasonable estimates of shoreline age because: (1) modern algae from the lake yield a $\Delta^{14}C$ of 108% modern (LDGO 1735 E, Table 1), indicating that the lake does not act as a significant reservoir for old carbon; (2) at one sub-surface exposure, tufa, dated at 9,780 ± 80 BP (LDGO 1735 O), is immediately overlain by *Chara* that dates at 9,480 ± 95 BP (ETH 5210). This suggests that secondary (post-depositional) contamination of tufa has been minimal, at least during the past 10 kyr.

Tufa also occurs as thin plates intercalated in laminated lacustrine sediments. In most cases $^{14}C$ assays on these tufa plates seem to provide reasonable ages of the host sediments. In two instances, however (both involving previously existing sediments that were reinundated), the tufa plates are clearly younger than the host sediments. We therefore assign less authority to dates from tufa plates, and assume that they provide only minimum ages on the host sediments.

Sections measured and logged along the Cardiel River, the Bayo River and Arroyo Cerro Gorro during the austral summers of 1987–88 and 1988–89 have been generalized in Fig. 1. Figure 2 depicts the inferred lake level fluctuations.

The oldest transgressional unit exposed in the walls of the stream cuts is composed of laminated silts and clays (Unit 1). Tufa collected from the underlying cobbles dates at $31{,}400^{+1{,}300}/_{-1{,}100}$ yr BP (LDGO 1714 X). Because of the antiquity of the tufa, and a lack of corroborating dates, we consider this a minimum age. Unit 1 can be traced to as high as +60 m in Arroyo Cerro Gorro. It may terminate and merge with the littoral embankment at +78 m, but this relationship is not proven. Unit 1 is overlain and partially truncated by alluvial sands and gravels (Unit 2) that are traceable lakeward to the +11-m level, indicating that the lake declined to or below that elevation during the regression following ~31,400 yr BP.

Evidence for a second transgression consists of a localized deposit of lacustrine silt (Unit 3) that overlies Unit 2. Tufa collected from the base of the silts at +12-m dates at 20,700 ± 320 yr BP (LDGO 1714 B), establishing a minimum date for the beginning of the transgression. Neither the timing nor the

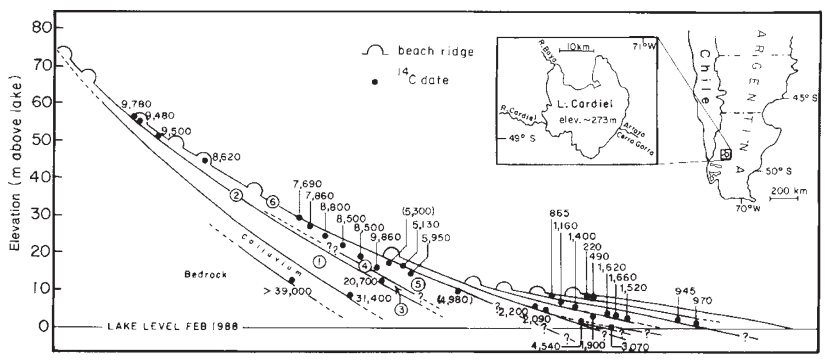


FIG. 1 Index map and composite stratigraphic section. Stratigraphy is generalized from sections exposed in stream cuts. Heavy lines represent regressional units and soils; areas between lines are transgressional units. No attempt has been made to portray realistically the unit thickness. Unit designations (circled numbers) are provided for discussion purposes only. Uncircled numbers are dates (yr BP).